Oxidative stress in oocytes during midprophase induces premature loss of cohesion and chromosome segregation errors

Adrienne T. Perkins[a], Thomas M. Das[a], Lauren C. Panzera[a], and Sharon E. Bickel[a,1]

[a]Department of Biological Sciences, Dartmouth College, Hanover, NH 03755

Edited by R. Scott Hawley, Stowers Institute for Medical Research, Kansas City, MO, and approved September 13, 2016 (received for review July 26, 2016)

In humans, errors in meiotic chromosome segregation that produce aneuploid gametes increase dramatically as women age, a phenomenon termed the "maternal age effect." During meiosis, cohesion between sister chromatids keeps recombinant homologs physically attached and premature loss of cohesion can lead to missegregation of homologs during meiosis I. A growing body of evidence suggests that meiotic cohesion deteriorates as oocytes age and contributes to the maternal age effect. One hallmark of aging cells is an increase in oxidative damage caused by reactive oxygen species (ROS). Therefore, increased oxidative damage in older oocytes may be one of the factors that leads to premature loss of cohesion and segregation errors. To test this hypothesis, we used an RNAi strategy to induce oxidative stress in *Drosophila* oocytes and measured the fidelity of chromosome segregation during meiosis. Knockdown of either the cytoplasmic or mitochondrial ROS scavenger superoxide dismutase (SOD) caused a significant increase in segregation errors, and heterozygosity for an *smc1* deletion enhanced this phenotype. FISH analysis indicated that SOD knockdown moderately increased the percentage of oocytes with arm cohesion defects. Consistent with premature loss of arm cohesion and destabilization of chiasmata, the frequency at which recombinant homologs missegregate during meiosis I is significantly greater in SOD knockdown oocytes than in controls. Together these results provide an in vivo demonstration that oxidative stress during meiotic prophase induces chromosome segregation errors and support the model that accelerated loss of cohesion in aging human oocytes is caused, at least in part, by oxidative damage.

meiosis | maternal age effect | oxidative damage | reactive oxygen species | superoxide dismutase

Chromosome segregation errors during female meiosis are the leading cause of birth defects and miscarriages in humans and their incidence increases dramatically with age (1). Over 90% of Down syndrome cases are the result of an extra copy of chromosome 21 inherited from the mother (2). Although the probability of a meiotic missegregation event is relatively low during a woman's twenties, by the time she reaches her early forties, she has a one in three chance of conceiving an aneuploid fetus (3). Work in the last decade has begun to shed light on the molecular mechanisms that underlie this phenomenon known as the "maternal age effect."

Proper chromosome segregation during both mitosis and meiosis requires that physical linkages between sister chromatids (cohesion) be formed, maintained, and released in a regulated manner (4, 5). Sister chromatid cohesion, mediated by the evolutionarily conserved cohesin complex, is established during DNA replication. During meiosis, in addition to holding sister chromatids together, cohesion is required to maintain the physical association of recombinant homologs and is therefore essential for proper segregation during the first as well as the second meiotic division (6–8). Normally, a crossover ensures proper segregation as long as cohesion distal to a crossover stabilizes the chiasma and keeps the four-chromatid bivalent intact (Fig. 1*A*). Cohesion-mediated association of homologous chromosomes promotes proper orientation and microtubule attachments on the meiosis I (MI) spindle. However, if arm cohesion is lost before spindle assembly, premature separation of homologs can result in segregation errors. In addition, centromeric cohesion must be protected during anaphase I to ensure that sisters remain associated until anaphase II.

The hypothesis that deterioration of meiotic cohesion over a woman's lifetime contributes to the maternal age effect has gained considerable support over the last decade (9, 10). One reason this theory is attractive is that in human oocytes, cohesion is established and meiotic recombination is completed during early fetal development. Oocytes then arrest in midprophase I (dictyate) until they are recruited for ovulation starting at puberty. Therefore, to maintain the physical association of homologs and promote accurate chromosome segregation, meiotic cohesion must remain intact for decades. Several lines of investigation have uncovered age-dependent cohesion defects in human oocytes as well as those of model organisms (8, 11–18). However, the mechanism(s) leading to loss of cohesion remains largely unexplored.

One hallmark of the aging cell is an increase in oxidative damage caused in large part by reactive oxygen species (ROS) (19–22). Produced primarily in the mitochondria as byproducts of metabolism, ROS can damage proteins, lipids, and DNA throughout the cell (22–25). Whereas low levels of ROS have been implicated in signaling pathways (25), failure to tightly control ROS levels can disrupt the redox status of the cell and result in oxidative stress (23). Such stress is thought to arise in aging cells due to their diminished ability to efficiently neutralize ROS (24, 26, 27) and there is strong evidence in different organisms and cell types that oxidative damage increases with age (26, 28–30). Given

Significance

Chromosome segregation errors during female meiosis, the leading cause of birth defects and miscarriages, increase dramatically as women age. Because oxidative damage increases with age and oocytes age during a woman's lifetime, one factor that may contribute to increased segregation errors in older women is damage of the protein linkages (cohesion) required for accurate segregation. In support of this hypothesis, we find that inducing oxidative stress in *Drosophila* oocytes during meiotic prophase causes a significant increase in segregation errors due to premature loss of cohesion. These data demonstrate that oxidative stress during the stage at which human oocytes remain arrested for decades can cause meiotic segregation errors and offer insight into why cohesion deteriorates with age.

Author contributions: A.T.P. and S.E.B. designed research; A.T.P., T.M.D., L.C.P., and S.E.B. performed research; A.T.P., T.M.D., and S.E.B. analyzed data; and A.T.P. and S.E.B. wrote the paper.

The authors declare no conflict of interest.

This article is a PNAS Direct Submission.

Freely available online through the PNAS open access option.

[1]To whom correspondence should be addressed. Email: sharon.e.bickel@dartmouth.edu.

This article contains supporting information online at www.pnas.org/lookup/suppl/doi:10.1073/pnas.1612047113/-/DCSupplemental.

the extensive aging that human oocytes experience during a woman's lifetime, accumulation of oxidative damage has been proposed as one factor that may contribute to the maternal age effect (27, 31–33), but so far only correlative evidence exists to support this theory.

Testing the hypothesis that oxidative stress can induce meiotic segregation errors requires an experimental system in which ROS levels can be manipulated and the effect on chromosome segregation measured. One way to increase ROS levels within the oocyte is to lower the level of ROS scavengers, which detoxify ROS and help maintain a physiologically safe redox state. The superoxide dismutase (SOD) family of enzymes provides an important defense against oxidative stress by catalyzing the reduction of superoxide to oxygen and hydrogen peroxide. Two cellular isoforms of SOD have been extensively characterized: cytoplasmic SOD1 (Cu/ZnSOD) and mitochondrial SOD2 (MnSOD). In flies and mice, a decrease in SOD activity in the whole organism can increase oxidative damage, reduce lifespan, and lower tolerance to exogenous sources of oxidative stress (34–43). Furthermore, SOD levels have been shown to decline with age (29, 44).

Here we test the hypothesis that elevated levels of ROS lead to chromosome segregation errors due to premature loss of cohesion. To mimic the age-dependent increase in oxidative damage that occurs naturally in the human oocyte, we performed conditional knockdown (KD) of ROS scavengers in the *Drosophila* oocyte. When we knock down either SOD1 or SOD2 during midprophase I, we observe a significant increase in chromosome nondisjunction (NDJ). In addition, meiotic segregation errors in SOD2 KD oocytes increase when the dosage of the cohesin subunit SMC1 is decreased. Direct analysis of cohesion using FISH revealed that arm cohesion defects are more prevalent in SOD KD oocytes than in controls. Consistent with premature loss of arm cohesion and destabilization of chiasmata, the relative frequency at which recombinant homologs missegregate during MI is significantly higher for SOD KD oocytes than for controls. These data provide in vivo evidence that oxidative stress can cause meiotic chromosome segregation errors due to premature loss of cohesion and destabilization of chiasmata. Our findings provide support for the hypothesis that oxidative damage in the aging oocyte contributes to the maternal age effect in humans.

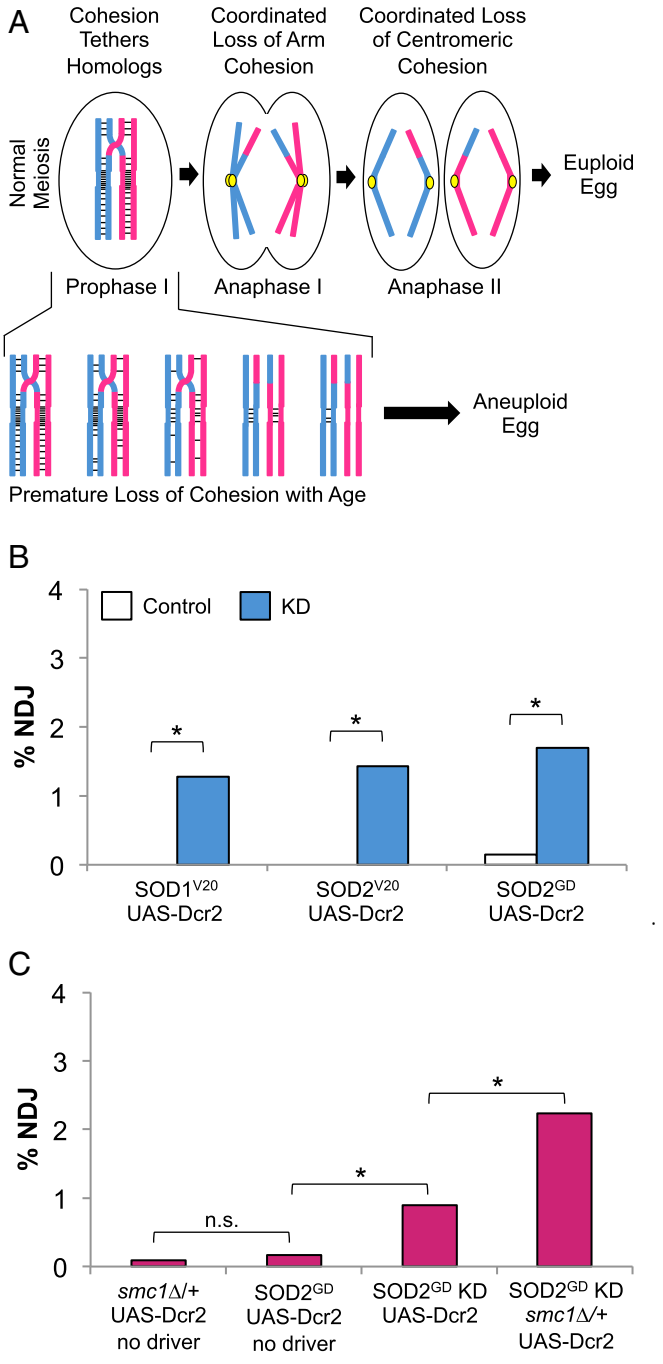

Fig. 1. SOD1 or SOD2 KD during midprophase I in *Drosophila* oocytes causes an increase in meiotic NDJ. (*A*) Cohesion is depicted by black bars between pink or blue sister chromatids. Accurate segregation depends on arm cohesion to hold recombinant homologs together until anaphase I and centromeric cohesin to hold sisters together until anaphase II. Premature loss of cohesion can lead to segregation errors and aneuploid eggs. (*B*) Percent NDJ for each SOD KD genotype and its respective control. *SI Appendix*, Table S1 provides raw data. (*C*) Percent NDJ for $SOD2^{GD}$ KD and control in wild type and *smc1Δ/+* backgrounds. *SI Appendix*, Table S5 provides raw data. For both *B* and *C*, we simultaneously drove expression of a UAS-Dicer-2 transgene to maximize the efficiency of the RNAi in germline cells. *$P < 0.025$, using the statistical test described in ref. 72.

Results

SOD KD Leads to Meiotic Chromosome Segregation Errors. To focus on the effect of oxidative stress in the oocyte, we used an inducible RNAi strategy to drive expression of SOD hairpins in the female germline (*SI Appendix*, Figs. S1*A* and S2*A*). Use of the mat-α-tubulin-GAL4-VP16 driver (matα driver) (45) allowed us to knock down either SOD1 or SOD2 in the female germline during midprophase I, well after cohesion establishment and the initiation of meiotic recombination (46). Because the *Drosophila* germline is somewhat resistant to RNAi (47), we simultaneously drove expression of an upstream activation sequence (UAS)-Dicer-2 transgene to maximize KD efficiency (46, 48, 49). We measured the fidelity of *X* chromosome segregation using our standard genetic assay (*SI Appendix*, Fig. S1*B*), which allows for the recovery of progeny resulting from aneuploid gametes and provides a quantitative readout of meiotic outcomes on a large scale. For all KD experiments, we compared meiotic NDJ in SOD KD females (with both the hairpin and driver transgenes) to that of control females (with the hairpin transgene but no driver).

To knock down SOD1, we used a transgene encoding the short hairpin $SOD1^{V20}$ (*SI Appendix*, Fig. S2*A*). The matα driver elicited robust KD of SOD1 protein in ovary extracts (*SI Appendix*, Fig. S2*B*). In addition, we detected a significant increase in oxidative damage in ovary extracts from SOD1 KD compared with control females (*SI Appendix*, Fig. S2*C*). When we assayed meiotic chromosome segregation, SOD1 KD in the ovary caused

a small but significant increase in NDJ (Fig. 1*B* and *SI Appendix*, Table S1*A*).

We also investigated the effect of SOD2 KD on chromosome segregation in *Drosophila* oocytes because mitochondria are the main producers of ROS in the cell and SOD2 is the primary scavenger of superoxide in the mitochondrial matrix (50). Moreover, several lines of evidence indicate that when SOD2 activity is decreased, elevation of ROS is not restricted to the mitochondria. Oxidative stress caused by partial loss of SOD2 has been shown to activate the mitochondrial permeability transition pore, which permits the release of small molecules, including ROS, from the mitochondrial matrix into the cytosol (51–53). Consistent with these observations, decrease of SOD2 has been demonstrated to impact cytosolic components (40) and cause fragmentation of nuclear DNA (54, 55). Therefore, we reasoned that SOD2 KD may also impact chromosome segregation.

RNAi hairpins targeting two different regions of the SOD2 transcript ($SOD2^{V20}$ and $SOD2^{GD}$, *SI Appendix*, Fig. S2*A*) each resulted in detectable KD in the ovary (*SI Appendix*, Fig. S2*B*) and also caused a significant increase in NDJ similar to that caused by SOD1 KD (Fig. 1*B* and *SI Appendix*, Table S1 *B* and *C*). Our observation that two different SOD2 hairpins as well as a SOD1 hairpin elicit similar outcomes argues that NDJ is not due to an RNAi off-site target. Based on these data, we conclude that oxidative stress in oocytes can negatively impact the fidelity of meiotic chromosome segregation, and that a decrease in mitochondrial or cytoplasmic SOD is sufficient to induce this effect.

SOD KD in a Sensitized Background Leads to Higher Levels of Meiotic NDJ, Consistent with Loss of Chiasmata. Because the NDJ that we observed in the above experiments was small, we wondered whether the achiasmate segregation system that operates in *Drosophila* oocytes might be masking the true effect of oxidative stress on meiotic chromosome segregation. This system relies upon pericentric heterochromatin-mediated association of homologs (Fig. 2*A*) to facilitate accurate segregation of bivalents that fail to achieve a crossover and are therefore "achiasmate" (56–59). One challenge with our SOD KD experiments is that the achiasmate system will not only ensure proper segregation of achiasmate bivalents but also recombinant homologs that fail to maintain chiasmata due to loss of arm cohesion (Fig. 2*A*) (11). Hawley and colleagues have previously shown that lowering the dosage of the Matrimony (Mtrm) protein using a P-element insertion allele ($mtrm^{KG08051}$) effectively disables the achiasmate segregation system (58). However, arm cohesion and chiasmata remain intact in $mtrm^{+/-}$ heterozygotes (60). Therefore, to more accurately assess the impact of SOD KD in oocytes, we repeated the above experiments in a $mtrm^{+/-}$ genetic background.

SOD KD in $mtrm^{+/-}$ oocytes resulted in considerably higher levels of NDJ. Fig. 2*B* shows the mean %NDJ values for two independent experiments performed for each SOD hairpin (*SI Appendix*, Tables S2–S4). When we decrease SOD1 levels in $mtrm^{+/-}$ oocytes we observe a significant increase in NDJ. The $SOD2^{V20}$ and $SOD2^{GD}$ hairpins elicited very similar phenotypes. Even in the absence of the UAS-Dicer2 transgene, the level of NDJ for all three KD genotypes is considerably higher in the $mtrm^{+/-}$ oocytes (Fig. 2*B*) than in a wild-type $mtrm^{+}$ background (Fig. 1*B*). The higher level of NDJ observed in control oocytes is not unexpected because a small fraction of *Drosophila X* chromosome bivalents are naturally achiasmate in *Drosophila* oocytes (61) and will segregate randomly in the $mtrm^{+/-}$ background. This experiment demonstrates that when either the mitochondrial or cytosolic SOD protein is knocked down, meiotic segregation errors are more prevalent in oocytes lacking a functional achiasmate segregation system. These results are consistent with the hypothesis that the oxidative stress that *Drosophila* oocytes experience as a result of SOD KD causes destabilization of chiasmata, rendering recombinant homologs dependent on the achiasmate segregation system for their accurate segregation.

Oxidative Stress Causes an Increase in Premature Loss of Arm Cohesion. Oxidative stress is likely to impact several pathways within the cell and damage of meiotic spindle components, kinetochores, or the spindle assembly checkpoint (SAC) could lead to meiotic segregation errors in older oocytes (62–65). However, because there is evidence that cohesion deteriorates with age (8, 11–18), and because NDJ is more pronounced when SOD is knocked down in $mtrm^{+/-}$ oocytes, we were specifically interested in examining the effect of oxidative stress on the integrity of meiotic cohesion.

If SOD KD leads to premature loss of cohesion, then oocytes with a reduced level of functional cohesin may be more susceptible to the effect of SOD KD on NDJ. To test this possibility, we used females heterozygous for a deletion of the *smc1* gene (*smc1Δ*/+) in which the protein level of the cohesin subunit SMC1 is lowered (11), but still adequate to support accurate meiotic chromosome segregation (11) (Fig. 1*C* and *SI Appendix*,

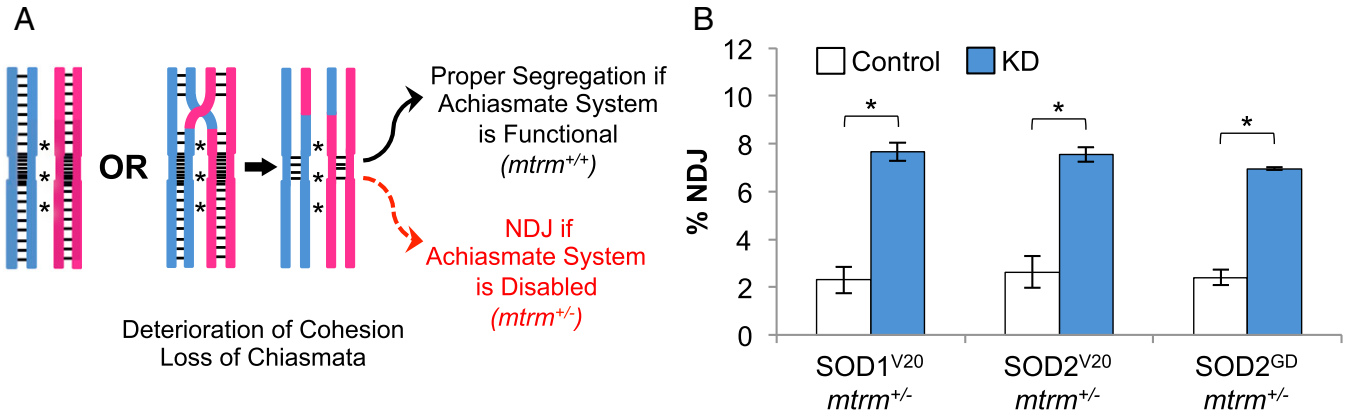

Fig. 2. SOD KD in a $mtrm^{+/-}$ background results in higher levels of NDJ, consistent with loss of chiasmata. (*A*) The achiasmate segregation system in *Drosophila* oocytes is mediated by heterochromatin interactions between the homologs, diagrammed here by asterisks. Homologs that fail to cross over as well as those that prematurely lose their chiasmata due to loss of arm cohesion will segregate properly when the achiasmate segregation system is functional. However, if the achiasmate system is disrupted by lowering the dosage of *mtrm*, then recombinant homologs that lose their chiasmata will be prone to missegregation. (*B*) Mean percent NDJ for each SOD KD genotype and its respective control in a $mtrm^{+/-}$ background. $^{*}P < 0.05$, using a *t* test, $n = 2$. Error bars represent SEM. *SI Appendix*, Tables S2–S4 provide raw data.

Table S5). Indeed, SOD2 KD in the ovaries of *smc1Δ*/+ females resulted in significantly more NDJ than SOD2 KD alone (Fig. 1*C* and *SI Appendix*, Table S5) consistent with the hypothesis that oxidative stress disrupts meiotic cohesion.

To directly assess the state of sister chromatid cohesion in SOD KD oocytes, we used *X*-chromosome FISH probes (Fig. 3*A*) to assay arm and pericentric cohesion in mature oocytes (a mixture of prometaphase I- and metaphase I-arrested oocytes). For each probe, an oocyte was scored as having a cohesion defect if three or four separated FISH signals were visible (Fig. 3*B*).

Interestingly, we observed a moderate increase in arm cohesion defects for all four KD genotypes that we examined, but pericentric cohesion defects were quite rare (Fig. 3*C* and *SI Appendix*, Fig. S3 and Table S6). Germline coexpression of the $SOD2^{V20}$ hairpin and UAS-Dicer-2 in flies that were wild type for matrimony ($mtrm^{+}$) resulted in an almost twofold increase in arm cohesion defects compared with control oocytes (1.88-fold increase, $P = 0.150$). Arm cohesion defects also were elevated when we used the same hairpin to knock down SOD2 in the $mtrm^{+/-}$ heterozygote (1.71-fold increase, $P = 0.194$). We attribute the somewhat weaker phenotype in the SOD2 KD $mtrm^{+/-}$ oocytes to less efficient KD in the absence of the UAS-Dcr2 transgene (which, for logistical reasons we cannot include). Importantly, the increase in arm cohesion defects was independent of the *mtrm* genotype examined. SOD1 KD in a $mtrm^{+/-}$ background elicited an increase in arm cohesion defects that was similar to that of SOD2 KD (1.91-fold increase, $P = 0.163$). The fact that all three SOD KD genotypes resulted in a 1.7- to 1.9-fold increase in arm cohesion defects strengthens the validity of these results. Although the moderate increase in arm cohesion defects for individual SOD2 or SOD1 tests did not satisfy the $P \leq 0.05$ criterion for significance, when we combine the data from all three SOD genotype pairs, we obtain a P value = 0.017. Moreover, the defects in SOD KD oocytes are on par with that observed when the cohesin subunit SMC3 is decreased using the short hairpin $SMC3^{V20}$ (3.2-fold increase, $P = 0.064$). Knockdown of SMC3 during meiotic prophase using this hairpin and the matα driver has previously been shown to induce meiotic segregation errors and missegregation of recombinant homologs due to premature loss of cohesion (46). Given how similar the FISH results of the three SOD KD genotypes are to each other and to those of the SMC3 KD oocytes, we conclude that increased levels of oxidative stress during meiotic prophase negatively impact the maintenance of arm cohesion in oocytes.

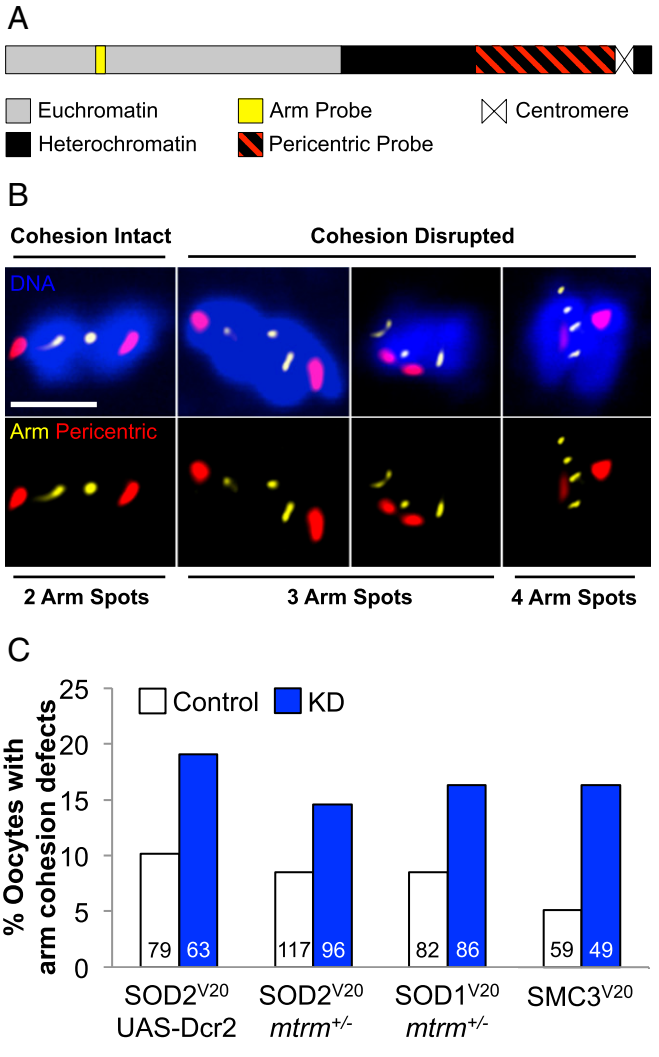

Fig. 3. FISH assay reveals that oxidative stress causes a moderate increase in premature loss of arm cohesion. (*A*) Diagram of the *Drosophila X* chromosome and probes used in FISH assay. (*B*) Representative images showing intact arm cohesion (two arm probe spots, one for each homolog), and disrupted arm cohesion (three to four arm probe spots, indicating separation of sister chromatid arms). Images are maximum projections of confocal *Z* series. (Scale bar, 2 μm.) (*C*) Percentage of mature oocytes with arm cohesion defects for each KD genotype and its respective control in the specified genetic background. The matα driver was used for all KD genotypes. Number of oocytes scored for each genotype is shown within each bar. *SI Appendix*, Table S6 provides raw data.

Intriguingly, the percentage of SOD1 or SOD2 KD oocytes in which we detect arm cohesion defects by FISH (14.6–19.0%, Fig. 3*C* and *SI Appendix*, Table S6) is approximately twofold higher than the NDJ values we observe for SOD KD in the $mtrm^{+/-}$ background (6.87–7.03%, Fig. 2*B* and *SI Appendix*, Tables S2–S4). These results would be expected if premature loss of arm cohesion and destabilization of chiasmata resulted in homologs that experienced random segregation during the first meiotic division. In other words, 50% of the affected bivalents would segregate accurately due to random chance.

Cohesion Defects Caused by Oxidative Stress Lead to Loss of Chiasmata and Missegregation of Recombinant Homologs During MI. Our FISH analysis provides evidence that arm cohesion is compromised by oxidative stress. We wanted to further test the hypothesis that the NDJ we observe in SOD KD oocytes arises (at least in part) because of premature loss of arm cohesion. Under normal circumstances, a crossover ensures the proper segregation of a bivalent during the first meiotic division because arm cohesion keeps the recombinant homologs physically associated (Fig. 1*A*). However, if arm cohesion deteriorates prematurely, loss of chiasmata may lead to missegregation of recombinant homologs because they have lost their physical connection to each other (Fig. 1*A*). If the moderate increase in arm cohesion defects detected in our FISH analysis of SOD KD oocytes has functional consequences, we should observe recombinant chromosomes missegregating at a higher frequency in SOD KD oocytes than in control oocytes. Therefore, we performed an additional "recombinational history" assay that allowed us to genotype the missegregating chromosomes (11, 46, 66).

One advantage of our NDJ test is that we can recover viable progeny that inherit two *X* chromosomes (Diplo-*X* females) from their mother due to NDJ (*SI Appendix*, Fig. S1*B*). Because females in the original NDJ test shown in Fig. 2*B* were heterozygous for visible markers along the *X* chromosome, we performed an additional cross with the Diplo-*X* females to genotype their *X* chromosomes and determine whether chromosomes that missegregated in the NDJ test had undergone one or more crossovers (*SI Appendix*, Fig. S1*C*). To compare the relative frequency at which recombinant bivalents missegregate in control and KD

genotypes, we divided the number of Diplo-*X* progeny that inherited at least one recombinant chromosome by the total number of progeny scored in the NDJ test and applied a multiplicity factor of 10^3 to make comparisons more straightforward (Fig. 4*A* and *SI Appendix*, Table S7).

When we genotyped the *X* chromosomes of the Diplo-*X* females from the experiments presented in Fig. 2*B* ($mtrm^{+/-}$ background), we observed a significant increase in the relative frequency at which recombinant bivalents missegregate in SOD KD oocytes compared with each matched control (Fig. 4*A* and *SI Appendix*, Table S7). Moreover, all three hairpins resulted in very similar frequencies of recombinant chromosome missegregation, indicating that a decrease in mitochondrial or cytosolic SOD results in similar meiotic outcomes. These data support the model that loss of cohesion caused by oxidative stress in the oocyte leads to loss of chiasmata and missegregation of recombinant chromosomes.

One trivial explanation for the finding that recombinant chromosomes missegregate more frequently when SOD is knocked down is that a decrease in SOD activity leads to an increase in crossovers. We verified that this was not the case by comparing the crossover frequency and distribution along the *X* chromosome in SOD KD and control oocytes and found that they are not dramatically different (*SI Appendix*, Fig. S4).

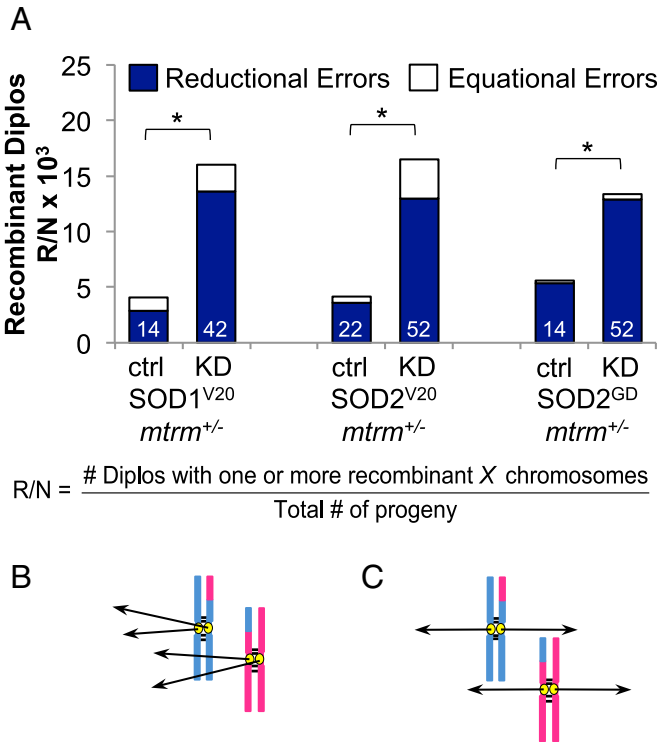

Fig. 4. Premature loss of arm cohesion in SOD KD oocytes causes an increase in the missegregation of recombinant homologs during MI. (*A*) Diplo-*X* females from Fig. 2*B* were genotyped and the frequency of recombinant bivalent missegregation (*R/N*) for each SOD KD genotype and its respective control is shown. $*P < 0.001$ for the total missegregation frequency, 2×2 χ^2 contingency test. The data for each genotype are subdivided into the frequency of reductional errors (Diplo-*X* females that inherited two homologs, $car^{+/-}$) and equational errors (Diplo-*X* females that inherited two sister chromatids, $car^{+/+}$ or $car^{-/-}$). Number of Diplo-*X* females genotyped is indicated within each bar. *SI Appendix*, Table S7 provides raw data. (*B* and *C*) Missegregation patterns consistent with our FISH and recombinational history data. (*B*) Chiasma destabilization allows homologs to segregate randomly in MI. (*C*) Chiasma destabilization followed by equational segregation of sister chromatids during MI and random segregation during MII.

Genotyping Diplo-*X* females for the centromere-proximal *car* marker in our recombinational history assay also allowed us to determine whether they harbored two homologs (reductional error) or two sister chromatids (equational error), typically indicative of premature loss of arm or centromeric cohesion, respectively. Strikingly, the vast majority of missegregation events in all genotypes were reductional errors (Fig. 4*A*). These data agree with those of our FISH analysis, which indicated that pericentric cohesion defects were quite rare (*SI Appendix*, Table S6).

Together, our data lead us to conclude that oxidative stress in the oocyte during meiotic prophase causes premature loss of arm cohesion that results in destabilization of chiasmata and missegregation of recombinant homologs during the first meiotic division. These findings are important because the majority of human trisomies that arise from maternally derived meiotic errors are reductional (3). Notably, our results support the model that increased oxidative damage in older oocytes contributes to the maternal age effect.

Discussion

Approximately 20 years ago, Tarín proposed that accumulation of oxidative damage in aging human oocytes may contribute to the maternal age effect (32). However, testing this hypothesis directly in human oocytes is virtually impossible. Using *Drosophila* as an experimental system has allowed us to manipulate levels of the ROS scavenger SOD in oocytes and determine whether oxidative stress impairs the fidelity of meiotic chromosome segregation. We find that a decrease of either cytoplasmic SOD1 or mitochondrial SOD2 in germline cells induces very similar consequences; meiotic segregation errors are significantly increased. These data represent an in vivo demonstration that oxidative stress in the oocyte can cause meiotic chromosome segregation errors. As such, our work has important implications when considering the physiological mechanisms that underlie the human maternal age effect.

Proteins that incur oxidative damage in the aging human oocyte are most likely numerous and disruption of several different pathways could contribute to segregation errors. However, our genetic and cytological evidence indicate that increased NDJ in SOD KD oocytes arises, at least in part, from premature loss of meiotic arm cohesion. An important consideration when interpreting our data is that the matα driver used to induce SOD KD does not turn on until well after meiotic S phase (46). Because meiotic cohesion is established normally, our experimental design allows us to look at the impact of oxidative stress specifically on the maintenance of meiotic cohesion. In addition, lowering the dosage of the cohesin subunit SMC1 enhances the NDJ phenotype of SOD2 KD oocytes, consistent with the model that oocytes with less functional cohesin are more vulnerable to the impact of oxidative stress. Moreover, by using FISH to directly examine cohesion in prometaphase I and metaphase I oocytes, we find that SOD KD causes a moderate increase in arm cohesion defects that is comparable to that of SMC3 KD oocytes. Recombinational history analyses confirm that the functional consequence of oxidative stress-induced loss of arm cohesion is destabilization of chiasmata, resulting in a significant increase in the frequency at which recombinant homologs missegregate during MI.

The finding that segregation errors increase when either the cytoplasmic or mitochondrial SOD enzyme is decreased reinforces our conclusion that the redox state of oocytes impacts meiotic sister chromatid cohesion. Several lines of evidence indicate that increased levels of ROS are not restricted to the mitochondria when SOD2 protein is decreased (51, 52, 54, 55). Therefore, it is likely that SOD2 KD also induces oxidative damage in the cytosol and nucleus. Moreover, opening of the mitochondrial permeability transition pore and release of small

molecules into the cytosol is stimulated when ROS levels in the mitochondrial matrix reach a threshold level (53). This phenomenon may help explain why two SOD2 hairpins that elicit different levels of KD (*SI Appendix*, Fig. S2*B*) still result in very similar levels of meiotic NDJ (Figs. 1*B*, 2*B*, and 4*A*).

Our results demonstrate that when oxidative stress is induced in the *Drosophila* oocyte, sister chromatid cohesion is less efficiently maintained. In at least some respects, our Gal4/UAS induction of oxidative stress during the normal oogenesis pathway is mimicking the increase in oxidative damage that occurs naturally within the aging human oocyte. One possibility is that cohesive linkages are lost prematurely because cohesin subunits are damaged by ROS. In addition, we have recently reported that active rejuvenation of meiotic cohesion occurs during meiotic prophase I in the *Drosophila* oocyte (46). Therefore, failure to maintain cohesion when SOD is knocked down may also be occurring because the players required for rejuvenation are damaged and rejuvenation efficiency declines. Interestingly, both our FISH and recombinational history data indicate that centromeric cohesion is less vulnerable to the effects of oxidative stress, at least within the time frame of meiotic prophase in *Drosophila* oocytes. It is possible that the compact state of heterochromatin makes cohesive linkages in this region less accessible to damaging ROS. Centromeric cohesion might also be relatively immune to oxidative stress-induced defects in our experiments because of the high density of cohesin rings within heterochromatin. Alternatively, variation in the rejuvenation of arm versus centromeric cohesion (46, 67) may result in different susceptibilities to oxidative stress.

We were surprised by the relatively high number of arm cohesion defects detected by FISH in SOD and SMC3 control oocytes. These were observed in both $mtrm^{+}$ and $mtrm^{+/-}$ oocytes and therefore we can exclude the possibility that heterozygosity for *mtrm* is eliciting premature loss of arm cohesion. Our scoring was quite stringent. To qualify as a defect, arm spots needed to be completely separated by a distance greater than or equal to the diameter of the spots. In many cases we detected two spots that were connected by a very thin chromatin thread; these instances were not counted as defects. We cannot rule out the possibility that some proportion of designated defects actually corresponded to arm foci that appeared to be completely separated but were in fact connected by a chromatin thread that was too faint to detect. However, our recombinational history analyses indicate that the majority of missegregating chromosomes in SOD control oocytes were recombinant, consistent with premature loss of arm cohesion leading to missegregation. Therefore, our data raise the possibility that a low level of arm cohesion defects occur in wild-type *Drosophila* oocytes but that these bivalents segregate accurately when the achiasmate segregation system is functional. Regardless of the baseline level of cohesion defects in SOD control oocytes, our experiments demonstrate that induction of oxidative stress during meiotic prophase causes an increase in both the incidence of arm cohesion defects and the missegregation of recombinant homologs during MI.

When SOD activity is decreased during meiotic prophase, we observe primarily reductional errors, which are indicative of homolog missegregation during MI. Our data are most consistent with random segregation of homologs during the first meiotic division (Fig. 4*B*). However, we cannot rule out the possibility that some fraction of SOD KD oocytes undergo reverse segregation as described by Hoffmann and colleagues for human oocytes (68) (Fig. 4*C*). Although age-dependent weakening of centromeric cohesion has been observed in mouse oocytes and proposed to result in segregation of nonsisters to the same pole during MI (10), our data indicate that this is not the primary mechanism underlying missegregation in *Drosophila* SOD KD oocytes.

Although our work indicates that meiotic cohesion is negatively affected by oxidative stress, the targets of oxidative damage in the aging human oocyte are most likely numerous and not limited to proteins that promote sister chromatid cohesion. Along these lines, we also observed a small (but insignificant) increase in the missegregation of presumed nonrecombinant bivalents in SOD KD oocytes (*SI Appendix*, Table S7). These missegregation events may be reflecting oxidative damage of other pathways such as spindle assembly, microtubule attachments, and/or the SAC, which would be expected to impact the segregation of both chiasmate and achiasmate bivalents.

Our finding that oxidative stress in the *Drosophila* oocyte negatively impacts the stability of sister chromatid cohesion and induces chromosome segregation errors provides mechanistic insight into how physiological changes during the aging process could contribute to the maternal age effect in humans. Although the risk factors that contribute to age-dependent NDJ errors are undoubtedly complex and premature loss of cohesion cannot explain all missegregation outcomes observed in human oocytes (1), it is consistent with certain types of trisomies, such as those that arise from chromosome 21 bivalents with a distally placed chiasmata (69–71). Furthermore, as women age, even bivalents with crossovers that are more proximal become susceptible to segregation errors (71), as would be expected if oxidative damage renders longer regions of the chromatid arms devoid of cohesion. A major advantage of our experimental system is the potential to identify oocyte proteins that are damaged by prolonged exposure to oxidative stress. Future studies that use such an approach will continue to broaden our understanding of both cohesion-dependent and -independent mechanisms that reduce the fidelity of meiotic chromosome segregation in older women.

Materials and Methods

Fly Stocks and Crosses. All flies were reared on a standard cornmeal molasses diet and kept at 25 °C. See *SI Appendix*, Table S8 for a complete list of stocks used to produce these data.

NDJ Assay. Because *Drosophila* can tolerate certain sex chromosome aneuploidies (*SI Appendix*, Fig. S1*B*), we measured meiotic chromosome missegregation using *Bar (B)*, a dominant *X* chromosome marker. B^{+} females were crossed to attached *X^Y, v f B* males. Progeny that arise from normal (*X*) as well as Diplo-*X* and Nullo-*X* gametes can be recovered and distinguished based on their sex and eye shape. Because all normal progeny survive but half of the exceptional progeny are not viable, (*XXX^Y* and *00*), %NDJ was calculated using the following formula: [(2(Diplos + Nullos))/(*n* + Diplos + Nullos)]100, where *n* is the number of total progeny scored. *P* values for individual NDJ tests were calculated as described in ref. 72. *P* values for mean %NDJ were calculated using a *t* test, $n = 2$. *P* values <0.05 were considered to be statistically significant.

Recombinational History Analysis of Diplo-*X* Females. To determine whether chromosomes had undergone recombination before missegregation in the NDJ assay (*SI Appendix*, Fig. S1*C*), single Diplo-*X* females from the NDJ tests were crossed to two *y w* males. By scoring their male progeny for the visible markers *sc*, *cv*, *f*, and *car*, we could infer the *X* chromosome genotype of each Diplo-*X* female.

For the recombinational history calculations, we combined the Diplo-*X* genotype information from two separate NDJ experiments because the NDJ values for paired experiments were very similar (*SI Appendix*, Tables S2–S4 and S7). To compare the relative frequency of recombinant chromosome missegregation in control and KD genotypes, we divided the number of Diplo-*X* progeny that inherited at least one recombinant chromosome (*R*) by the total number of progeny scored in the NDJ test (*N*) and multiplied by 10^3 to make comparisons easier. Only females that were fertile and that could be assigned a definitive genotype were included in the analysis. Thus, the number of females genotyped may be fewer than the number of Diplo-*X* females recovered in the NDJ tests. Note that a direct comparison of NDJ values and recombination history numbers is not possible because the %NDJ was calculated by doubling the number of Diplo-*X* and Nullo-*X* progeny (see above), so our genotype analysis of actual Diplo-*X* females represents only a subset of the reported NDJ events. *P* values were calculated using a two-tailed 2×2 χ^2 contingency test with Yates' correction. A *P* value <0.05 was considered to be statistically significant.

One limitation of our recombinational history assay is that it may underestimate the number of bivalents that have incurred at least one crossover.

Because we can only genotype two of the four chromatids for any bivalent, when a Diplo-*X* female contains two nonrecombinant *X* chromosomes, we cannot rule out the possibility that these arose from a bivalent with a crossover that did not involve these two chromatids. In addition, the markers associated with our transgenes limit the number of visible markers that we can use on the *X* chromosome. Therefore, one interval within the marked *X* chromosome is quite large (*cv-f*), and double crossovers within this region would be invisible to us.

Carnation (*car*) is our most centromere proximal visible marker but is still 3.5 cM distal to *bobbed*, which resides within the centromere proximal heterochromatin of the *X* chromosome. Therefore, in a very small number of cases, it is possible that a Diplo-*X* female that is homozygous for the *car* allele could actually correspond to a reductional exception for which one of the chromatids sustained a crossover between *car* and heterochromatin.

Crossover Frequency Analysis. SOD KD and control females were crossed to *y w* males and crossovers along the *X* chromosome were measured for three intervals (*sc-cv*, *cv-f*, and *f-car*) by scoring their male progeny.

Immunoblot Analysis of SOD1 and SOD2 Levels in Ovary Extracts. For each genotype, 15 μg of total ovary extract was separated by SDS/PAGE on a 4–20% gradient gel (BioRad) and transferred to PVDF membrane (Millipore). The blot was cut horizontally to allow for separate processing for SOD and tubulin antibodies. The following primary antibodies and concentrations were used: 1:500 rabbit anti-SOD1 (Abcam, ab13498), 1:2,000 rabbit anti-SOD2 (Abcam, ab13534), and 1:5,000 monoclonal mouse anti–α-tubulin, DM1A (Sigma, T9206). Promega goat anti-rabbit or goat anti-mouse secondary antibodies were used at 1:7,500. Blots were incubated with Lumi-Phos chemiluminescence substrate (Thermo Scientific) and imaged using the ChemiDoc Touch system (BioRad). Signals were quantified using Image Lab software (BioRad). SOD signal was normalized to tubulin and mean SOD protein levels relative to the control were calculated using two separate blots.

Quantification of Oxidative Damage in SOD1 KD and Control Ovary Extracts. SOD1 control and KD ovaries were dissected in 1× modified Robb's solution (73) supplemented with antioxidants [100 μM diethylenetriaminepentaacetic acid (DTPA) and 1 mM butylated hydroxytoluene (BHT)]. Ovaries were homogenized in extraction buffer [1× PBS, 0.5% SDS, 1 mM BHT, 100 μM DTPA, and 1× HALT protease inhibitors (Pierce) including 1 mM EDTA], centrifuged at 3,000 × *g* for 5 min and the supernatant was filtered through a 0.22-μm Millipore Millex GV filter PVDF to remove lipids. One-tenth volume of 10% (wt/vol) streptozocin (Sigma) was added to the homogenate, the sample was incubated at room temperature for 15 min, and centrifuged at 3,000 × *g* for 5 min. The supernatant protein concentration was assayed using a Nanodrop 2000 (ThermoFisher) and adjusted to 0.5 mg/mL by adding extraction buffer. Following addition of one-fifth volume of 10 mM DNPH (in 2N HCl), the sample was incubated for 60 min at room temperature. An equal volume of 20% TCA was added and the sample was incubated on ice for 10 min. Following centrifugation at 1,000 × *g* for 10 min, the pellet was washed with a 1:1 mixture of ethanol:ethyl acetate and sonicated to disperse the pellet. Centrifugation and wash steps were repeated two times. After a final spin, the pellet was dissolved (with sonication) in buffer containing 20 mM Tris·HCl pH 6.8, 0.2% SDS, and 2 M urea. Protein concentration was measured (BioRad DC assay) and 5 μg of protein was separated on a 4–20% gradient stain-free gel (BioRad). Immunoblotting and analysis was performed as described above with the following exceptions. The stain-free gel was activated to reveal total protein before transfer, the blot was imaged with the ChemiDoc Touch system to reveal the total protein/lane after transfer, and Immunu-Star AP chemiluminescence substrate (BioRad) was used. Rabbit anti-DNP (CellBio Labs, 230801) was used at a dilution of 1:2,000. For each lane, DNP signal was normalized to total protein (post-transfer), and mean normalized DNP signal (oxidatively damaged proteins) relative to the control was calculated using three separate blots, and a *P* value was calculated using a *t* test, $n = 3$. A *P* value of <0.05 was considered to be statistically significant.

FISH. Ovaries from 20 to 25 fattened females were dissected and fixed as previously described (74). Following fixation, ovaries were rinsed in 1× PBS, 0.5% BSA, 0.1% Triton X-100, transferred to a shallow dissecting dish, and late-stage egg chambers were detached from earlier stages by pipetting with a BSA-coated pipette tip. Chorions and vitelline membranes of late-stage oocytes were manually removed as described in ref. 75. Oocytes were nutated for 2 h at room temperature in 1× PBS and 1% Triton X-100 containing 100 μg/mL RNase (ThermoFisher Scientific). In situ hybridization was performed as previously described (74). The hybridization solution contained 2.5 ng/μl of a Cy3-labeled pericentric probe (5′-Cy3-AGGGATCGTTAG-CACTCGTAAT; Integrated DNA Technologies) and Alexa 647 end-labeled fragments were prepared from six BAC clones at a final concentration of 0.31 pmol fluor/μL. The pericentric oligonucleotide probe hybridizes to the 359-bp satellite repeat, which comprises ∼11 Mb of the *X* chromosome heterochromatin. The six BAC clones (BACR17C09, BACR06J12, BACR35J16, BACR20K01, BACR35A18, and BACR26L11; BAC PAC Resources) hybridize to the *X* chromosome arm at cytological region 6E-7B. The arm probe was prepared as described in ref. 76.

Images were acquired using a 40× oil Plan Fluor DIC (N.A. 1.3) objective with 4× digital zoom on a Nikon A1RSi laser scanning confocal microscope. *Z* series (0.25-μm step) were captured using unidirectional scanning with a 407-nm laser (for DAPI), a 561-nm laser (for Cy3), and a 640-nm laser (for Alexa 647) using parameters that were best suited for each individual oocyte. *Z* stacks were cropped, deconvolved, and contrast enhanced using Volocity 6.3 software (Perkin-Elmer) with parameters that were best suited for each image. Maximum intensity projections of *Z* series are shown in Fig. 3. Cohesion defects were scored by examining *Z* stacks in three dimensions using Volocity. The number of arm and pericentric foci colocalizing with the DAPI signal were tabulated for each oocyte. For each probe, an oocyte was scored as having a cohesion defect if three to four individual spots were detected. An arm or centromere signal was considered to be individual if the spot was separated in all three dimensions by at least the diameter of the smallest spot counted. After the first round of scoring, oocytes with possible cohesion defects were also scored by a second person who was "blind" to the genotype. *P* values were calculated using a two-tailed Fisher's exact test. A *P* value of <0.05 was considered to be statistically significant.

ACKNOWLEDGMENTS. We thank Kathryn Cottingham for helpful discussions about statistical analysis and data presentation; Ann Lavanway for confocal microscopy help; Charlotte Jeffreys, Elizabeth Morse, and Brittany Toffey for technical support; and Viji Subramanian, Roger Sloboda, and members of the S.E.B. laboratory for critical reading of the manuscript. We are grateful to the Bloomington Stock Center at Indiana University for providing fly stocks used in this study. Trangenic RNAi stocks were generated by the Transgenic RNAi Project (TRiP) at Harvard Medical School (NIH/National Institute of General Medical Sciences R01-GM084947) and the Vienna *Drosophila* RNAi Center (48). This work was funded by NIH Grant GM59354 (to S.E.B.).

1. Nagaoka SI, Hassold TJ, Hunt PA (2012) Human aneuploidy: Mechanisms and new insights into an age-old problem. *Nat Rev Genet* 13(7):493–504.
2. Freeman SB, et al. (2007) The National Down Syndrome Project: Design and implementation. *Public Health Rep* 122(1):62–72.
3. Hassold T, Hunt P (2001) To err (meiotically) is human: The genesis of human aneuploidy. *Nat Rev Genet* 2(4):280–291.
4. Peters JM, Nishiyama T (2012) Sister chromatid cohesion. *Cold Spring Harb Perspect Biol* 4(11):a011130.
5. McNicoll F, Stevense M, Jessberger R (2013) Cohesin in gametogenesis. *Curr Top Dev Biol* 102:1–34.
6. Bickel SE, Orr-Weaver TL, Balicky EM (2002) The sister-chromatid cohesion protein ORD is required for chiasma maintenance in Drosophila oocytes. *Curr Biol* 12(11):925–929.
7. Buonomo SB, et al. (2000) Disjunction of homologous chromosomes in meiosis I depends on proteolytic cleavage of the meiotic cohesin Rec8 by separin. *Cell* 103(3):387–398.
8. Hodges CA, Revenkova E, Jessberger R, Hassold TJ, Hunt PA (2005) SMC1beta-deficient female mice provide evidence that cohesins are a missing link in age-related nondisjunction. *Nat Genet* 37(12):1351–1355.
9. Herbert M, Kalleas D, Cooney D, Lamb M, Lister L (2015) Meiosis and maternal aging: Insights from aneuploid oocytes and trisomy births. *Cold Spring Harb Perspect Biol* 7(4):a017970.
10. Chiang T, Schultz RM, Lampson MA (2012) Meiotic origins of maternal age-related aneuploidy. *Biol Reprod* 86(1):1–7.
11. Subramanian VV, Bickel SE (2008) Aging predisposes oocytes to meiotic nondisjunction when the cohesin subunit SMC1 is reduced. *PLoS Genet* 4(11):e1000263.
12. Chiang T, Duncan FE, Schindler K, Schultz RM, Lampson MA (2010) Evidence that weakened centromere cohesion is a leading cause of age-related aneuploidy in oocytes. *Curr Biol* 20(17):1522–1528.
13. Liu L, Keefe DL (2008) Defective cohesin is associated with age-dependent misaligned chromosomes in oocytes. *Reprod Biomed Online* 16(1):103–112.
14. Lister LM, et al. (2010) Age-related meiotic segregation errors in mammalian oocytes are preceded by depletion of cohesin and Sgo2. *Curr Biol* 20(17):1511–1521.
15. Angell R (1997) First-meiotic-division nondisjunction in human oocytes. *Am J Hum Genet* 61(1):23–32.
16. Duncan FE, et al. (2012) Chromosome cohesion decreases in human eggs with advanced maternal age. *Aging Cell* 11(6):1121–1124.

17. Tsutsumi M, et al. (2014) Age-related decrease of meiotic cohesins in human oocytes. *PLoS One* 9(5):e96710.
18. Yun Y, Lane SI, Jones KT (2014) Premature dyad separation in meiosis II is the major segregation error with maternal age in mouse oocytes. *Development* 141(1):199–208.
19. Muller FL, Lustgarten MS, Jang Y, Richardson A, Van Remmen H (2007) Trends in oxidative aging theories. *Free Radic Biol Med* 43(4):477–503.
20. Guarente L, Kenyon C (2000) Genetic pathways that regulate ageing in model organisms. *Nature* 408(6809):255–262.
21. Sohal RS (2002) Role of oxidative stress and protein oxidation in the aging process. *Free Radic Biol Med* 33(1):37–44.
22. Finkel T, Holbrook NJ (2000) Oxidants, oxidative stress and the biology of ageing. *Nature* 408(6809):239–247.
23. Dumollard R, Carroll J, Duchen MR, Campbell K, Swann K (2009) Mitochondrial function and redox state in mammalian embryos. *Semin Cell Dev Biol* 20(3):346–353.
24. Stadtman ER (2001) Protein oxidation in aging and age-related diseases. *Ann N Y Acad Sci* 928:22–38.
25. Holmström KM, Finkel T (2014) Cellular mechanisms and physiological consequences of redox-dependent signalling. *Nat Rev Mol Cell Biol* 15(6):411–421.
26. Sohal RS, Weindruch R (1996) Oxidative stress, caloric restriction, and aging. *Science* 273(5271):59–63.
27. Tarín JJ (1996) Potential effects of age-associated oxidative stress on mammalian oocytes/embryos. *Mol Hum Reprod* 2(10):717–724.
28. Orr WC, Sohal RS (1994) Extension of life-span by overexpression of superoxide dismutase and catalase in Drosophila melanogaster. *Science* 263(5150):1128–1130.
29. Tian L, Cai Q, Wei H (1998) Alterations of antioxidant enzymes and oxidative damage to macromolecules in different organs of rats during aging. *Free Radic Biol Med* 24(9): 1477–1484.
30. Sohal RS, Agarwal A, Agarwal S, Orr WC (1995) Simultaneous overexpression of copper- and zinc-containing superoxide dismutase and catalase retards age-related oxidative damage and increases metabolic potential in Drosophila melanogaster. *J Biol Chem* 270(26):15671–15674.
31. Agarwal A, Aponte-Mellado A, Premkumar BJ, Shaman A, Gupta S (2012) The effects of oxidative stress on female reproduction: A review. *Reprod Biol Endocrinol* 10:49.
32. Tarín JJ (1995) Aetiology of age-associated aneuploidy: A mechanism based on the 'free radical theory of ageing'. *Hum Reprod* 10(6):1563–1565.
33. Devine PJ, Perreault SD, Luderer U (2012) Roles of reactive oxygen species and antioxidants in ovarian toxicity. *Biol Reprod* 86(2):27.
34. Duttaroy A, Paul A, Kundu M, Belton A (2003) A Sod2 null mutation confers severely reduced adult life span in Drosophila. *Genetics* 165(4):2295–2299.
35. Paul A, et al. (2007) Reduced mitochondrial SOD displays mortality characteristics reminiscent of natural aging. *Mech Ageing Dev* 128(11–12):706–716.
36. Phillips JP, Campbell SD, Michaud D, Charbonneau M, Hilliker AJ (1989) Null mutation of copper/zinc superoxide dismutase in Drosophila confers hypersensitivity to paraquat and reduced longevity. *Proc Natl Acad Sci USA* 86(8):2761–2765.
37. Martin I, Jones MA, Grotewiel M (2009) Manipulation of Sod1 expression ubiquitously, but not in the nervous system or muscle, impacts age-related parameters in Drosophila. *FEBS Lett* 583(13):2308–2314.
38. Kirby K, Hu J, Hilliker AJ, Phillips JP (2002) RNA interference-mediated silencing of Sod2 in Drosophila leads to early adult-onset mortality and elevated endogenous oxidative stress. *Proc Natl Acad Sci USA* 99(25):16162–16167.
39. Li Y, et al. (1995) Dilated cardiomyopathy and neonatal lethality in mutant mice lacking manganese superoxide dismutase. *Nat Genet* 11(4):376–381.
40. Lebovitz RM, et al. (1996) Neurodegeneration, myocardial injury, and perinatal death in mitochondrial superoxide dismutase-deficient mice. *Proc Natl Acad Sci USA* 93(18): 9782–9787.
41. Elchuri S, et al. (2005) CuZnSOD deficiency leads to persistent and widespread oxidative damage and hepatocarcinogenesis later in life. *Oncogene* 24(3):367–380.
42. Melov S, et al. (1999) Mitochondrial disease in superoxide dismutase 2 mutant mice. *Proc Natl Acad Sci USA* 96(3):846–851.
43. Muller FL, et al. (2006) Absence of CuZn superoxide dismutase leads to elevated oxidative stress and acceleration of age-dependent skeletal muscle atrophy. *Free Radic Biol Med* 40(11):1993–2004.
44. Tatone C, et al. (2006) Age-dependent changes in the expression of superoxide dismutases and catalase are associated with ultrastructural modifications in human granulosa cells. *Mol Hum Reprod* 12(11):655–660.
45. Januschke J, et al. (2002) Polar transport in the Drosophila oocyte requires Dynein and Kinesin I cooperation. *Curr Biol* 12(23):1971–1981.
46. Weng KA, Jeffreys CA, Bickel SE (2014) Rejuvenation of meiotic cohesion in oocytes during prophase I is required for chiasma maintenance and accurate chromosome segregation. *PLoS Genet* 10(9):e1004607.
47. Ni JQ, et al. (2011) A genome-scale shRNA resource for transgenic RNAi in Drosophila. *Nat Methods* 8(5):405–407.
48. Dietzl G, et al. (2007) A genome-wide transgenic RNAi library for conditional gene inactivation in Drosophila. *Nature* 448(7150):151–156.
49. Lee YS, et al. (2004) Distinct roles for Drosophila Dicer-1 and Dicer-2 in the siRNA/miRNA silencing pathways. *Cell* 117(1):69–81.
50. Holley AK, Bakthavatchalu V, Velez-Roman JM, St Clair DK (2011) Manganese superoxide dismutase: Guardian of the powerhouse. *Int J Mol Sci* 12(10):7114–7162.
51. Cui H, Kong Y, Zhang H (2012) Oxidative stress, mitochondrial dysfunction, and aging. *J Signal Transduct* 2012:646354.
52. Kokoszka JE, Coskun P, Esposito LA, Wallace DC (2001) Increased mitochondrial oxidative stress in the Sod2 (+/–) mouse results in the age-related decline of mitochondrial function culminating in increased apoptosis. *Proc Natl Acad Sci USA* 98(5): 2278–2283.
53. Zorov DB, Juhaszova M, Sollott SJ (2014) Mitochondrial reactive oxygen species (ROS) and ROS-induced ROS release. *Physiol Rev* 94(3):909–950.
54. Muid KA, Karakaya HÇ, Koc A (2014) Absence of superoxide dismutase activity causes nuclear DNA fragmentation during the aging process. *Biochem Biophys Res Commun* 444(2):260–263.
55. Van Remmen H, et al. (2003) Life-long reduction in MnSOD activity results in increased DNA damage and higher incidence of cancer but does not accelerate aging. *Physiol Genomics* 16(1):29–37.
56. Karpen GH, Le MH, Le H (1996) Centric heterochromatin and the efficiency of achiasmate disjunction in *Drosophila* female meiosis. *Science* 273(5271):118–122.
57. Dernburg AF, Sedat JW, Hawley RS (1996) Direct evidence of a role for heterochromatin in meiotic chromosome segregation. *Cell* 86(1):135–146.
58. Harris D, et al. (2003) A deficiency screen of the major autosomes identifies a gene (matrimony) that is haplo-insufficient for achiasmate segregation in Drosophila oocytes. *Genetics* 165(2):637–652.
59. Hawley RS, et al. (1992) There are two mechanisms of achiasmate segregation in Drosophila females, one of which requires heterochromatic homology. *Dev Genet* 13(6):440–467.
60. Xiang Y, et al. (2007) The inhibition of polo kinase by matrimony maintains G2 arrest in the meiotic cell cycle. *PLoS Biol* 5(12):e323.
61. Ashburner M, Golic K, Hawley R (2005) *Drosophila: A Laboratory Handbook* (Cold Spring Harbor Lab Press, Cold Spring Harbor, NY), 2nd Ed.
62. Handyside AH (2012) Molecular origin of female meiotic aneuploidies. *Biochim Biophys Acta* 1822(12):1913–1920.
63. Battaglia DE, Goodwin P, Klein NA, Soules MR (1996) Influence of maternal age on meiotic spindle assembly in oocytes from naturally cycling women. *Hum Reprod* 11(10):2217–2222.
64. Steuerwald N, Cohen J, Herrera RJ, Sandalinas M, Brenner CA (2001) Association between spindle assembly checkpoint expression and maternal age in human oocytes. *Mol Hum Reprod* 7(1):49–55.
65. Shomper M, Lappa C, FitzHarris G (2014) Kinetochore microtubule establishment is defective in oocytes from aged mice. *Cell Cycle* 13(7):1171–1179.
66. Koehler KE, et al. (1996) Spontaneous *X* chromosome MI and MII nondisjunction events in *Drosophila melanogaster* oocytes have different recombinational histories. *Nat Genet* 14(4):406–414.
67. Gyuricza MR, et al. (2016) Dynamic and stable cohesins regulate synaptonemal complex assembly and chromosome segregation. *Curr Biol* 26(13):1688–1698.
68. Ottolini CS, et al. (2015) Genome-wide maps of recombination and chromosome segregation in human oocytes and embryos show selection for maternal recombination rates. *Nat Genet* 47(7):727–735.
69. Lamb NE, et al. (1996) Susceptible chiasmate configurations of chromosome 21 predispose to non-disjunction in both maternal meiosis I and meiosis II. *Nat Genet* 14(4): 400–405.
70. Oliver TR, et al. (2008) New insights into human nondisjunction of chromosome 21 in oocytes. *PLoS Genet* 4(3):e1000033.
71. Lamb NE, Sherman SL, Hassold TJ (2005) Effect of meiotic recombination on the production of aneuploid gametes in humans. *Cytogenet Genome Res* 111(3–4): 250–255.
72. Zeng Y, Li H, Schweppe NM, Hawley RS, Gilliland WD (2010) Statistical analysis of nondisjunction assays in Drosophila. *Genetics* 186(2):505–513.
73. Theurkauf WE, Hawley RS (1992) Meiotic spindle assembly in Drosophila females: Behavior of nonexchange chromosomes and the effects of mutations in the *nod* kinesin-like protein. *J Cell Biol* 116(5):1167–1180.
74. Giauque CC, Bickel SE (2016) Heterochromatin-associated proteins HP1a and Piwi collaborate to maintain the association of achiasmate homologs in Drosophila Oocytes. *Genetics* 203(1):173–189.
75. McKim KS, Joyce EF, Jang JK (2009) Cytological analysis of meiosis in fixed Drosophila ovaries. *Methods Mol Biol* 558:197–216.
76. Nguyen HQ, et al. (2015) Drosophila casein kinase I alpha regulates homolog pairing and genome organization by modulating condensin II subunit Cap-H2 levels. *PLoS Genet* 11(2):e1005014.